RAPID COMMUNICATIONS

PHYSICAL REVIEW B VOLUME 44, NUMBER 9 1 SEPTEMBER 1991-I

Formation of virtual ordered states along a phase-decomposition path

Long-Qing Chen and A. G. Khachaturyan
Department of Mechanics and Materials Science, Rutgers University, Piscataway, New Jersey 08855
(Received 29 April 1991)

The temporary appearance of a virtual ordered phase during a decomposition reaction is discussed in terms of thermodynamics and illustrated by a computer simulation that simultaneously describes ordering, clustering, and coarsening. It is particularly shown that the virtual ordered phase may temporarily appear within a miscibility gap during the decomposition of a homogeneous disordered phase into a mixture of two disordered phases. In such systems, an ordered phase existing along the interfaces between the two equilibrium disordered phases proves to be thermodynamically stable at low temperatures and an interfacial order-disorder phase transition is predicted. The possibility that the ordered phases observed in epitaxial layers of ternary and quaternary III-VI compound semiconductors and SiGe could be virtual phases is discussed.

An isostructural decomposition of a disordered phase into a mixture of two disordered phases within a miscibility gap of an equilibrium phase diagram is one of the simplest solid-state transformations in materials. It is generally believed that during an isostructural decomposition, only atomic clustering can occur. Inside the spinodal curve, atomic clustering results in development of solute-poor and solute-rich phase regions until their compositions reach the equilibrium ones determined by the equilibrium phase diagram. It will be shown below that this is not necessarily always the case. Ordering and disordering transitions may accompany the atomic clustering, which results in one of the two phases temporarily having an ordered structure prior to formation of two equilibrium disordered phases. We will call such ordered phases "virtual" ordered phases.

Thermodynamically, virtual ordered states are expected when some segments of their free-energy curves lie below the corresponding segments of the free energy of the as-quenched disordered state. This situation is schematically illustrated by Fig. 1 where the free energies of the disordered and ordered phases are plotted as a function of composition. The free energy of the ordered phase describes a dependence of the free energy minima with respect to the long-range order (LRO) parameter on composition. As shown in Fig. 1, free energies of an ordered single phase between compositions C' and C'' are lower than those of the disordered state at the same compositions, but they are above the common tangent line describing the free energy of a mixture of two equilibrium disordered phases. Kinetically, however, virtual ordered states should be revealed during decomposition since ordering always occurs much faster than the competing decomposition process whose diffusional length is much longer.

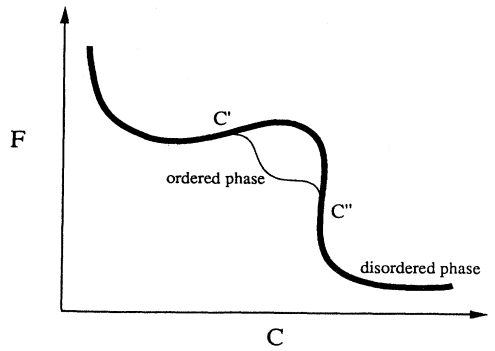

FIG. 1. Schematic dependence of the free energies of ordered (thin line) and disordered (thick line) phases on composition.

To illustrate the sequence of the structural transformation in a system characterized by the free energy depicted in Fig. 1, we employed a computer simulation technique based on the microscopic kinetic theory,[1,2]

$$\frac{dn(\mathbf{r},t)}{dt}=\sum_{\mathbf{r}'}L_0(\mathbf{r}-\mathbf{r}')\frac{\delta F}{\delta n(\mathbf{r}',t)} \tag{1}$$

where $n(\mathbf{r},t)$ is the occupation probability for the solute atom B to be at a crystal lattice site $\mathbf{r}$ at the time t, $L_0(\mathbf{r}-\mathbf{r}')$ is the matrix of kinetic coefficients whose elements are probabilities of an elementary diffusional jump from site $\mathbf{r}$ to $\mathbf{r}'$ during the time unit, and F is the total free energy of the system. This kinetic equation particularly describes decomposition in a prototype system with a miscibility gap which is considered below. Its main advantage is that it describes automatically all important processes such as clustering, ordering, antiphase domain boundary (APB) migration, and coarsening.

Equation (1) is solved in the reciprocal space using the Euler method. Diffusion jumps are allowed only between nearest-neighbor lattice sites and we assume that the jumping probability over a unit of time (e.g., 1 s) is a constant (L_1). Reduced time is then measured in terms of typical time of an elementary diffusion event, i.e., $t^*=L_1t$, where t is a real time. The solution to Eq. (1) gives the occupation probability on each lattice site, which contains all the information concerning atomic structures and morphologies of a system.

It is emphasized that the main feature of a prototype system under consideration, which predetermines its kinetic and thermodynamic behavior, is the dependence of the free energy on composition shown in Fig. 1. In this respect, any free-energy model which provides such a dependence can be utilized to describe the decomposition kinetics. Particularly, we use the mean-field free energy

which is the simplest microscopic model resulting in a free-energy curve geometry shown in Fig. 1.

We consider a particular model binary alloy in a two-dimensional (2D) square lattice with the following set of interchange energies: $W_1=0.75$ eV, $W_2=-0.8$ eV, $W_3=-0.60$ eV, $W_4=-0.5$ eV, $W_5=-0.20$ eV, where W_1, W_2, W_3, W_4, and W_5 are the first-, second-, third-, fourth-, and fifth-neighbor effective interaction energies, respectively. The equilibrium state of the particular model system is a disordered phase at high temperatures and a mixture of two disordered phases at low temperatures as shown by the phase diagram in Fig. 2. In the phase diagram, T^* is the reduced temperature, $k_BT/|V(0)|$, where $V(0)$ is the value of $V(\mathbf{k})$, the Fourier transform of $W(\mathbf{r})$, at $\mathbf{k}=0$, and k_B is the Boltzmann constant. The thick line is the equilibrium phase boundary describing the miscibility gap, and the dotted line is the spinodal line. An important feature, which predetermines the free-energy dependence shown in Fig. 1, is an existence of a congruent order$\rightleftharpoons$disorder transition line which lies below the spinodal and is shown by a dot-dashed line. This line actually has nothing to do with the equilibrium diagram, but it characterizes free energies of nonequilibrium states. The existence of such a congruent order$\rightleftharpoons$disorder transition line dramatically affects the decomposition kinetics of a disordered phase into two disordered phases. It results in occurrence of a virtual ordered phase during an isothermal decomposition preceding the formation of the equilibrium mixture of two disordered phases.

For the computer simulation, two specific compositions within the two-phase field are selected to demonstrate the formation kinetics of virtual ordered phases along the decomposition path. They are shown by points *a* and *b* in Fig. 2. For both cases, the starting as-quenched state is a completely disordered alloy with every lattice site having an occupation probability equal to the average composition with a small random perturbation. The "aging" temperature is $T^*=0.11$. Free energies for both the ordered and disordered phases at the aging temperature are plotted in Fig. 3 as a function of composition. The computer simulation cell consists of 64×64 real space unit cells. Periodic boundary conditions are applied in both directions. The temporal morphological evolutions are shown in Figs. 4 and 5 in which the occupation probabilities are represented by gray levels. The higher the occupation probability is, the darker the gray level. However, in both Figs. 4(a) and 4(b), contrast has been exaggerated because of the small concentration inhomogeneities at the initial state of decomposition.

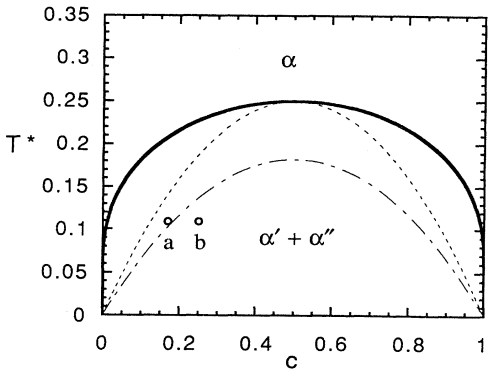

FIG. 2. Phase diagram of the model system. The thick line, dotted line, and dot-dashed line represent the miscibility gap, spinodal, and congruent order$\rightleftharpoons$disorder transition lines, respectively. T^* is the reduced temperature and c is the composition.

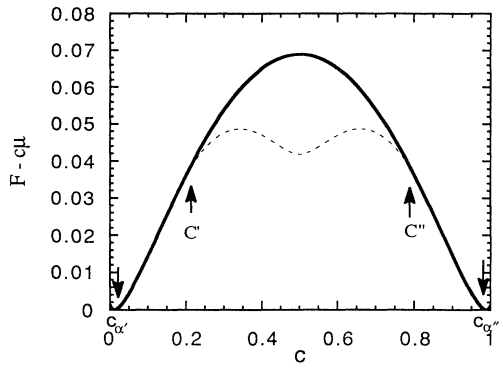

FIG. 3. Free energies of ordered and disordered phases at the reduced temperature $T^*=0.11$. The thick line represents the free energy of the disordered phase and the dotted line represents the free energy of the ordered phase. $C_{\alpha'}$ and $C_{\alpha''}$ are equilibrium compositions. C' and C'' are branching points between which the free energy of an ordered phase is lower than that of a disordered phase. μ is the chemical potential, C is the composition, and F is the Helmholtz free energy normalized by $V(0)$.

Composition c = 0.175. This composition is shown as point *a* in the phase diagram. For this composition, the isothermal aging starts from a slow isostructural spinodal

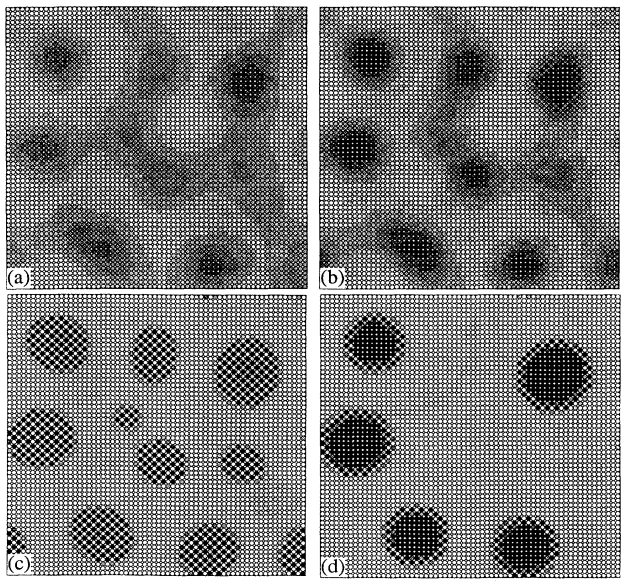

FIG. 4. Temporal evolution of occupation probabilities for an alloy with a composition $c=0.175$. (a) $t^*=370$; (b) $t^*=460$; (c) $t^*=470$; (d) $t^*=800$. Different values of occupation probabilities are represented by gray levels. The completely dark gray level represents $n(\mathbf{r})=1.0$ and the completely white gray level represents $n(\mathbf{r})=0.0$.

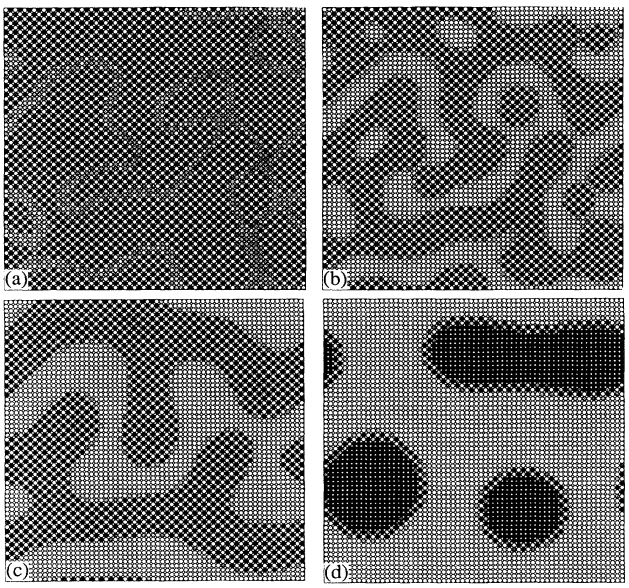

FIG. 5. Temporal evolution of occupation probabilities for an alloy with a composition $c=0.25$. (a) $t^*=5.0$; (b) $t^*=25$; (c) $t^*=100$; (d) $t^*=800$. The representation of occupation probabilities is the same as Fig. 4.

decomposition. Shown in Fig. 4(a) is a morphology during the decomposition at time $t^*=370$. Unlike usual spinodal decomposition in which both phases change their compositions without any crystallographic symmetry changes, the solute-rich phase here undergoes an ordering transition caused by the composition change towards its solubility limit. The region where this process occurs is shown in Fig. 4(b) ($t^*=460$). At $t^*=470$ the system already consists of a mixture of the solute-rich virtual ordered phase which appears as spherical precipitates and the solute-poor disordered phase which appears as a matrix [Fig. 4(c)]. Further aging of the two-phase mixture leads to the disappearance of the virtual ordered phase. The microstructure of the resultant equilibrium two-phase mixtures, is shown in Fig. 4(d) for time $t^*=800$. It is interesting to see in Fig. 4(d) that the boundary regions between these two equilibrium disordered phases stay ordered.

Composition $c=0.25$. This composition is indicated by point b in the phase diagram. In this case, instead of isostructural spinodal decomposition of the disordered phase expected from the equilibrium phase diagram, we have here first a congruent ordering transition which produces a virtual ordered phase, a nonstoichiometric ordered single-phase state with the composition is approximately the same as the initial disordered state. The virtual ordered phase contains antiphase domain boundaries (APB's) as shown in Fig. 5(a) at time $t^*=5.0$. Decomposition of the ordered single-phase produces the equilibrium disordered phase mainly along the APB's [Fig. 5(b), time $t^*=25$]. By time $t^*=100$ the system is already a mixture of the solute-rich virtual ordered phase and the solute-poor disordered phase [Fig. 5(c)]. After prolonged aging of this two-phase mixture, the virtual ordered phase disorders and its composition reaches that of the equilibrium solute-rich disordered phase [Fig. 5(d), time $t^*=800$]. The boundary regions between these two equilibrium disordered phases, however, stay ordered.

Above computer simulation for an idealized 2D binary alloy clearly demonstrates that virtual order may occur and later disappear during isothermal aging even if the equilibrium phase diagram dictates decomposition of the disordered phase into two disordered phases. The above considered model system displays two interesting sequence of phase transformations: (i) isostructural decomposition $\rightarrow$ virtual ordering (when a composition of solute-rich regions attains the critical composition of the congruent ordering described by a dot-dashed line curve in Fig. 2) $\rightarrow$ decomposition into ordered+disordered two-phase mixture $\rightarrow$ disordering of the virtual ordered phase; (ii) congruent ordering resulting in the virtual ordered phase $\rightarrow$ decomposition into ordered+disordered two-phase mixture $\rightarrow$ disordering of the virtual phase.

Another interesting phenomenon which was discovered during the course of this investigation is an order $\rightleftharpoons$disorder transformation at interfaces which is manifested by an occurrence of layers of a stable ordered phase on interfaces between two equilibrium disordered phases [Figs. 4(d) and 5(d)]. This can be easily understood if we examine the free-energy curves in Fig. 3. As shown in Fig. 3, the free energy of the ordered phase is lower than that of the disordered phase within a concentration range, $[C',C'']$, located between the two equilibrium concentrations $C_{\alpha'}$ and $C_{\alpha''}$. A homogeneous alloy with a composition within the range $[C',C'']$ cannot be at equilibrium since its free energy is higher than that of a mixture of $\alpha'+\alpha''$ phases. This is, however, not the case at boundaries where the composition is forced to assume all intermediate values between $C_{\alpha'}$ and $C_{\alpha''}$. The composition profile at boundaries, therefore, includes compositions within the range, $[C',C'']$, where the ordered phase is more stable than the disordered one. Therefore, ordering in these regions can be predicted from the thermodynamics as well. Increase in temperature above the congruent ordering line would result in an interfacial disordering. Therefore, an order$\rightleftharpoons$disorder transition at interfaces in an equilibrium mixture of *two disordered* phases can be observed upon heating or cooling the alloy across the congruent order$\rightleftharpoons$disorder transition temperature.

The conclusions drawn above from the thermodynamic analysis and a computer simulation of the kinetics for an idealized model are quite general. They are applied to any real system whose free energy has a similar geometry as that shown in Fig. 1. A simplified 2D model system, discussed here, is just a convenient simple example of a prototype system illustrating this behavior. The model, however, has an advantage that the kinetics and thermodynamics can easily be analyzed quantitatively. It is emphasized that some observed phenomena might be interpreted in terms of virtual ordering. For example, ordering occurs in molecular-beam-epitaxy grown epitaxial layers of ternary and quaternary III-V compound semiconductors[3] which otherwise decompose into two disordered phases when they are grown at more equilibrium conditions, e.g., from the melt. It was concluded that the ex-

istence of LRO in such systems is not thermodynamically favorable, at least in $Ga_xIn_{1-x}P$.[4] Therefore, the observed ordered phases may be regarded as virtual phases. We would also like to note that there is a reason to believe that ordered structures observed in thick and unstrained epilayers of the SiGe semiconductor alloy grown at about 400 °C (Ref. 5) (the alloy is supposed to undergo an isostructural decomposition[6,7]) are virtual ordered phases of this kind. This is also consistent with the fact that SiGe grown at a higher temperature (about 600 °C) does not order.[8] Such a behavior could be explained if the congruent order⇌disorder transition line in SiGe is somewhere between 400 and 600 °C.

In summary, our computer simulation clearly demonstrates that even for the case of an isostructural decomposition of a quenched disordered phase into two disordered phases, ordering and disordering transition may occur during decomposition. Depending on the aging temperature and the average composition of the quenched disordered phase, a virtual ordered phase may appear at the very beginning or at the intermediate states of a decomposition. It is shown that in such systems an interfacial order⇌disorder transition should occur by heating and cooling a mixture of two disordered phases across the low-temperature congruent ordering line.

The authors gratefully acknowledge support from the National Science Foundation under Grant No. NSF-DMR-88-17922. The computer simulation was performed on Cray-YMP at the Pittsburgh Supercomputing Center.

[1]A. G. Khachaturyan, Fiz. Tverd. Tela (Leningrad) **9**, 2594 (1967) [Sov. Phys. Solid State **9**, 2040 (1968)].

[2]A. G. Khachaturyan, *Theory of Structural Transformations in Solids* (Wiley, New York, 1983).

[3]S. Mahajan, M. A. Shahid, and D. E. Laughlin, in *Microscopy of Semiconducting Materials 1989,* Proceedings of the Royal Microscopical Society Conference, edited by A. G. Cullis and J. L. Hutchinson, IOP Conf. Proc. No. 100 (Institute of Physics and Physical Society, London, 1989), Sec. 3, p. 143.

[4]M. Kondow, H. Kakibayashi, T. Tanaka, and S. Minagawa, Phys. Rev. Lett. **63**, 884 (1989).

[5]F. K. LeGoues, V. P. Kesan, and S. S. Iyer, Phys. Rev. Lett. **64**, 40 (1990).

[6]V. N. Romanenko and V. I. Romanov-Omsky, Dokl. Akad. Nauk SSSR **129**, 553 (1959) [Sov. Phys. Dokl. **4**, 1342 (1959)].

[7]Ya. Umansky, V. Prilepskii, and S. Gorelik, Fiz. Tverd. Tela (Leningrad) **7**, 3310 (1965) [Sov. Phys. Solid State **7**, 2673 (1965)].

[8]T. S. Kuan, S. S. Iyer, and E. M. Yeo, in *Proceedings of the Forty-Seventh Annual Meeting of the Electron Microscopy Society of America,* edited by G. W. Bailey (San Francisco, San Francisco, 1989), p. 580.